

Boundary quantum criticality in models of magnetic impurities coupled to bosonic baths

Serge Florens,¹ Lars Fritz,² and Matthias Vojta²

¹ *Institut Néel, CNRS and Université Joseph Fourier, BP 166, 38042 Grenoble, France*

² *Institut für Theoretische Physik, Universität zu Köln, Zùlpicher Str. 77, 50937 Köln, Germany*

(Dated: March 23, 2007)

We investigate quantum impurity problems, where a local magnetic moment is coupled to the spin density of a bosonic environment, leading to bosonic versions of the standard Kondo and Anderson impurity models. In a physical situation, these bosonic environments can correspond either to deconfined spinons in certain classes of Z_2 frustrated antiferromagnets, or to particles in a multicomponent Bose gas (in which case the spin degree of freedom is attributed to hyperfine levels). Using renormalization group techniques, we establish that our impurity models, which feature an exchange interaction analogous to Kondo impurities in Fermi liquids, allow the flow towards a stable strong-coupling state. Since the low-energy bosons live around a single point in momentum space, and there is no Fermi surface, an impurity quantum phase transition occurs at intermediate coupling, separating screened and unscreened phases. This behavior is qualitatively different from previously studied spin-isotropic variants of the spin-boson model, which display stable intermediate-coupling fixed points and no screening.

PACS numbers: 75.20.Hr, 74.70.-b

I. INTRODUCTION

The investigation of quantum phase transitions in strongly correlated electronic systems has been an active field of research during the last two decades.¹ Recently, there has been growing interest in so-called impurity quantum phase transitions – these correspond to qualitative changes in the ground-state properties of discrete degrees of freedom (a spin 1/2 in the simplest case) upon changing their couplings to an external environment. On the one hand, impurity quantum phase transitions can be realized, e.g., in mesoscopic systems, such as quantum dot devices, which provide the high tunability required to access the transition point. On the other hand, the study of impurity problems is motivated through the dynamical mean-field theory^{2,3} (DMFT), which maps lattice models of strongly correlated electrons – assuming a momentum-independent self energy – onto effective self-consistent impurity models. In this language, certain bulk quantum phase transition correspond to impurity transitions in Anderson or Kondo-type models.

Impurity quantum phase transition occur in different contexts and setups. One possibility is a single magnetic impurity coupled to an unconventional fermionic host. A paradigmatic example being the so-called pseudogap Kondo model,⁴ originally motivated by the study of magnetic impurities in d -wave superconductors, where a spin 1/2 is coupled to the spin density of fermionic quasiparticles with a power-law density of states (DOS), $\rho(\omega) \propto |\omega|^r$. The lack of low-energy states (as compared to the standard Kondo model⁵) causes a competition between the local-moment dynamics and the formation of a strong-coupling ground state and leads to rich quantum critical behavior.^{4,6–8} Other fermionic impurity models display quantum phase transitions due to the competition between differently screened states, with

the two-channel Kondo^{9,10} and the two-impurity Kondo models^{11–13} being popular examples. The majority of these models were recently reviewed in Ref. 14.

Quantum impurities with a *bosonic* environment constitute a distinct class of models which can feature quantum phase transitions as well. A well-studied model is the spin-boson model, originally introduced to capture dissipation effects at the quantum level. Here, a generic two-level system (dubbed spin) is subject to the competing influence of a transverse field (causing tunneling between the two levels) and a longitudinally-coupled set of harmonic oscillators (providing friction). In the case of ohmic dissipation, this results in a Kosterlitz-Thouless phase transition at zero temperature, tuned by a variation of the dissipation strength.¹⁵ Note that the ohmic spin-boson model is equivalent to a Kondo model with anisotropic spin exchange terms, and hence does not constitute a distinct universality class. (This is different for sub-ohmic damping, see Refs. 14,16.) The topic of impurities in quantum magnets has motivated studies of the so-called Bose-Kondo model (which may also be viewed as a spin-isotropic spin-boson model with zero transverse field) – this model has a stable intermediate-coupling fixed point and no screening;^{17–21} this will be reviewed briefly in Sec. III. We note that the above-mentioned bosonic impurity models can be extended to include a fermionic environment as well, resulting in Bose-Fermi Kondo Hamiltonians, where the interactions of the impurity with the bosonic and fermionic baths compete.^{22–26} Models of this type have been proposed to describe quantum criticality in heavy-fermion compounds within extended DMFT,²² and could as well be realized in certain quantum-dot setups.²⁷

We have recently introduced²⁸ a distinct class of SU(2)-symmetric bosonic impurity models, where the environment consists of spin-1/2 objects, i.e., spinons con-

stituting the elementary excitations of certain frustrated quantum magnets. In contrast to the spin-boson type models mentioned above, where the environment always plays the role of a fluctuating (classical) magnetic field, our models display true quantum dynamics and allow singlet formation accompanied by complete screening.

The purpose of this paper is to give a comprehensive renormalization group (RG) analysis of various versions of these bosonic Kondo models, thus providing details which were left out in the short report of Ref. 28: (i) The first example concerns the elementary bosonic excitations (spinons) in the Z_2 spin-liquid state of a triangular Heisenberg model.²⁹ This model will be shown to display an impurity quantum phase transition, bearing some resemblance to the fermionic pseudogap Kondo model. (ii) A second example that follows the same philosophy concerns the setup of a “magnetic impurity” embedded in an optical lattice filled with a multicomponent bosonic gas.^{30,31} Here, the bosons are not collective modes originating from an underlying magnetic state, but are rather real bosonic atoms. In both cases, we derive the relevant quantum-field theory and study it using RG combined with epsilon expansion techniques. Although the structure of the theories is reminiscent of fermionic Kondo models, there are important differences: we demonstrate the importance of potential-scattering effects at the impurity location as well as the influence of bulk interactions.

Note that this paper will only study the RG flow at weak coupling; for situations with runaway flow to strong coupling – indicative of true screening – different techniques need to be applied. We have demonstrated this in Ref. 28, using strong-coupling toy models and large- N techniques; this will not be repeated here. Furthermore, we restrict our attention to situations where the bulk state does not break a local symmetry, i.e. we focus on paramagnetic phases including the quantum critical points.

The plan of the paper is as follows. In Sec. II we summarize the order-parameter description of nearly-critical antiferromagnets, distinguishing collinear and non-collinear ordering. In the non-collinear case of interest to us, deconfined bosonic spinons²⁹ emerge which correspond to fractional spin 1/2 excitations in a Z_2 spin liquid phase.^{32–34} In Sec. III we review the results of earlier work^{17–19} on a magnetic moment in a collinear antiferromagnet, described by a conventional ϕ^4 theory with triplon excitations, leading to a spin-isotropic spin-boson-like model without screening. Sec. IV is devoted to the central topic of this paper, namely the physics of a magnetic impurity in a Z_2 spin liquid. We present a microscopic derivation of the impurity action, which we analyze by RG methods, extending our earlier calculation²⁸ to two-loop level. Furthermore we propose a way to properly incorporate the bulk interactions using a mapping to an effective bosonic Anderson impurity model. Finally, in Sec. V we study how an impurity two-level system couples to an atomic gas of canonical bosons carrying an

internal degree of freedom (pseudospin). Again, we determine the phase diagram and critical properties using RG. A brief outlook will close the paper. Details of the RG calculations are deferred to the appendices. There, we also point out that the RG flow derived in Sec. V is identical to the one of a fully asymmetric fermionic Kondo model, which may arise in the DMFT context.

II. FIELD THEORIES OF NEARLY-CRITICAL QUANTUM ANTIFERROMAGNETS

Different types of magnetic Mott insulators naturally call for different types of order-parameter theories to describe the physics near the transition towards the symmetry-broken phase. In general, introducing an order parameter ϕ for the magnetic fluctuations near the ordering wavevector \vec{K} , a gradient expansion of the action naturally leads to a standard multicomponent ϕ^4 theory (or a non-linear sigma model). However, care is required for non-collinear spin correlations, as shown below.

Assuming a magnetic order characterized by a single ordering wave vector \vec{K} , the local spin operators can be parametrized as

$$\vec{S}_i = \Re \left(\vec{\phi} e^{i\vec{K} \cdot \vec{x}_i} \right) = \vec{n}_1 \cos(\vec{K} \cdot \vec{x}_i) + \vec{n}_2 \sin(\vec{K} \cdot \vec{x}_i), \quad (1)$$

where \vec{x}_i denotes the position of lattice site i , and $\vec{\phi}(\vec{x}, \tau) = \vec{n}_1 + i\vec{n}_2$ is a complex vector field in spin space which describes the order-parameter direction and varies slowly in space and time.

A. Collinear magnetic order

For a state with static collinear order we have fixed vectors $\vec{n}_{1,2}$ with $\vec{n}_1 \times \vec{n}_2 = 0$; the $\langle \vec{S}_i \rangle$ in Eq. (1) on all sites i point parallel or antiparallel w.r.t. a common axis. The undoped insulator La_2CuO_4 is of this type (if we neglect the small spin canting due to Dzyaloshinski-Moriya interactions), with in-plane ordering wave-vector $\vec{K} = (\pi, \pi)$ (the lattice spacing is unity here and in the following). For this specific value of \vec{K} on a square lattice the order parameter is independent of \vec{n}_2 .

Near quantum criticality, one is lead to the usual $O(3)$ quantum ϕ^4 theory in imaginary time:

$$\mathcal{S}_b = \int d^d x d\tau \left[|\partial_x \vec{\phi}|^2 + |\partial_\tau \vec{\phi}|^2 + g_0 (\vec{\phi}^2)^2 \right]. \quad (2)$$

For $\vec{K} = (\pi, \pi)$ the vector field $\vec{\phi}$ is now *real*; for commensurate \vec{K} , $\vec{\phi}$ is complex, but the phase degree of freedom is gapped. This theory has been studied at length in the literature,^{1,29} and its critical properties are relevant for the quantum phase transition from a Néel state to a

gapped paramagnet in several classes of unfrustrated antiferromagnets such as the bilayer square-lattice Heisenberg model and coupled spin-ladder models.

For general incommensurate \vec{K} , one has to parametrize $\vec{\phi} = \vec{n}e^{i\Theta}$, with a real vector \vec{n} and a phase field Θ . Interesting critical behavior may obtain here³⁵, which is not in the focus of this paper.

B. Non-collinear magnetic order

Non-collinear order is present if $\vec{n}_1 \times \vec{n}_2 \neq 0$ in (1); the order may be coplanar or fully three-dimensional. The former situation is e.g. realized in triangular quantum antiferromagnets, where the $\langle \vec{S}_i \rangle$ now lie in a plane in spin space, rather than along a single axis.

The simplest case of a non-collinear ordered state is the one where

$$\vec{n}_1 \cdot \vec{n}_2 = 0 \quad ; \quad \vec{n}_1^2 = \vec{n}_2^2 = 1, \quad (3)$$

corresponding to a spin spiral. An elegant way to resolve the constraints is via a parametrization of the order parameter according to³²

$$\vec{\phi} = \vec{n}_1 + i\vec{n}_2 = \epsilon_{\sigma\sigma'} z_{\sigma'} \frac{\vec{\sigma}_{\sigma\sigma'}}{2} z_{\sigma}, \quad (4)$$

with the single constraint $\sum_{\sigma} |z_{\sigma}|^2 = 1$ (here $\sigma = \uparrow, \downarrow$), $\vec{\sigma}$ is the vector of Pauli matrices, and $\epsilon_{\sigma\sigma'}$ is the fully antisymmetric matrix. The objects z_{σ} represent complex numbers (and hence are not canonical bosons), they describe a mapping from the four-dimensional unit sphere S_3 to S_2 . Obviously, this representation is unique up to a local Z_2 transformation $z_{\sigma} \rightarrow \eta z_{\sigma}$ with $\eta = \pm 1$.

Thus, in the non-collinear case described by (3,4), the long-distance fluctuations near a magnetic quantum critical point are described by a quantum field theory in terms of bosonic spinons:³²

$$\begin{aligned} \mathcal{S} = & \frac{1}{g} \int d^d x d\tau (|\partial_x z_{\sigma}|^2 + |\partial_{\tau} z_{\sigma}|^2) \\ & + \int d^d x d\tau \kappa(x, \tau) \left(\sum_{\sigma} |z_{\sigma}|^2 - 1 \right) \end{aligned} \quad (5)$$

where the integration over the auxiliary field κ enforces the constraint on $\sum_{\sigma} |z_{\sigma}|^2$. In Eq. (5) an additional Z_2 gauge field, corresponding to the above-mentioned gauge redundancy, has been omitted – this is justified provided that the gauge field is in a deconfined phase with massive fluctuations, which is the case for the triangular antiferromagnet. Note that the paramagnetic phase of (5) is a Z_2 spin liquid with gapped, deconfined bosonic spinons.^{32–34}

Let us note here that the fluctuations in a *collinear* magnet may also be written in terms of bosonic spinons, leading to a Schwinger boson representation:^{36,37}

$$\vec{S}(\vec{x}) = \sum_{\sigma, \sigma'} z_{\sigma}^*(\vec{x}) \frac{\vec{\sigma}_{\sigma\sigma'}}{2} z_{\sigma'}(\vec{x}), \quad (6)$$

with the constraint $\sum_{\sigma} |z_{\sigma}|^2 = 1$. Note the difference with Eq. (4): in contrast to the non-collinear case, the accompanying gauge redundancy here is of $U(1)$ symmetry. In such a situation, the gauge-field fluctuations are massless and cannot be ignored in a proper description of the bulk magnetism. The associated compact gauge theory is in general confining,³⁸ implying that bosonic spinons are bound in pairs and leading to the standard ϕ^4 theory (2) for triplon fluctuations.³⁹

$U(1)$ spin liquids with deconfined spinons may nevertheless arise: a special situation here are so-called deconfined critical points,⁴⁰ where a description in terms of bosonic spinons coupled to a non-compact $U(1)$ gauge field applies (which implies the suppression of hedgehogs⁴¹). Impurities characterized by a gauge charge and embedded in a $U(1)$ spin liquid have been studied in Ref. 42; the interplay with a magnetic impurity moment would be interesting to study, but is beyond the scope of the present paper.

III. A MAGNETIC IMPURITY IN A QUANTUM ANTIFERROMAGNET WITH COLLINEAR ORDER

Magnetic impurities embedded in a nearly critical collinear quantum antiferromagnet were analyzed in detail in Refs. 17–21. The bulk action \mathcal{S}_b (2), describing the physics close to the transition between the ordered Néel state and the disordered spin-gap state, is supplemented by the coupling to an impurity quantum spin $1/2 \vec{S}$, leading to:

$$\begin{aligned} \mathcal{S} = & \mathcal{S}_b + \mathcal{S}_{\text{imp}} + \mathcal{S}_{\text{Berry}}[\vec{S}], \\ \mathcal{S}_{\text{imp}} = & \gamma_0 \int d\tau \vec{S}(\tau) \cdot \vec{\phi}(\vec{x} = 0, \tau) \end{aligned} \quad (7)$$

where $\vec{\phi}(\vec{x}, \tau)$ is the real order-parameter field of (2), and $\mathcal{S}_{\text{Berry}}[\vec{S}]$ encodes the dynamics of the impurity spin \vec{S} . A weak-coupling RG analysis^{17,18} leads to the RG beta function for the dimensionless impurity coupling γ :

$$\beta(\gamma) = \frac{d\gamma}{d \ln \mu} = -\frac{\epsilon\gamma}{2} + \gamma^3 + \frac{5g^2\gamma}{144} \quad (8)$$

where $\epsilon = 3 - d$, μ is a renormalization scale, and the sign of the beta function is such that negative terms are RG relevant in the infrared. In Eq. (8), g denotes the renormalized bulk coupling in \mathcal{S}_b (2) which flows as in the standard ϕ^4 theory.⁴³ From Eq. (8) one finds a fixed-point value of the impurity coupling as $\gamma^{*2} = \epsilon/2 + \mathcal{O}(\epsilon^2)$. The critical fluctuations of the bulk plus impurity problem are thus controlled by a fixed point with couplings g^* (bulk) and γ^{*2} (impurity), which are both of order ϵ , i.e., perturbatively accessible near $d = 3$ bulk dimensions.

Most importantly, the flow of γ (8) near γ^* is infrared stable (!), in sharp contrast to (for example) the impurity quantum critical point of the pseudogap Kondo

model.^{4,7,8} The absence of runaway flow in Eq. (8) suggests the absence of a strong-coupling phase with complete screening, even at the bulk critical point with gapless bosonic modes. In a sense, this is not unexpected, as Eq. (7) describes the classical fluctuations of an effective magnetic field coupled to the impurity, being unable to quench the entropy.

As a consequence of (8), no quantum phase transitions occur in the model (7). The impurity properties are controlled by a stable intermediate-coupling fixed point, which describes a non-trivially fluctuating fractional-spin state. Near this fixed point, the impurity susceptibility and entropy obey¹⁸

$$\lim_{T \rightarrow 0} T \chi_{\text{imp}} = \mathcal{C}_1(d), \quad \lim_{T \rightarrow 0} S_{\text{imp}} = \mathcal{C}_2(d). \quad (9)$$

with universal constants $\mathcal{C}_1(d)$, $\mathcal{C}_2(d)$ (which depend on dimensionality d and impurity spin size S only). We note that the problem of an impurity in a collinear magnet can equivalently be formulated using a non-linear sigma model for the bulk¹⁹ – this leads to an expansion in $\epsilon = d - 1$, with similar impurity properties. Thus, the fractional-spin state is present for all $1 < d < 3$ – for $d = 2$ the field-theoretic predictions^{18,19} have been verified by extensive Quantum Monte Carlo simulations.^{20,21}

Paranthetically, we note that the fixed point at γ^* is unstable w.r.t. breaking of the underlying $SU(2)$ symmetry: a stable intermediate-coupling fixed point still exists in the XY case, whereas flow to strong coupling occurs in the Ising situation.^{24,25}

IV. A MAGNETIC IMPURITY IN A Z_2 SPIN LIQUID

As above, we intend to couple a magnetic impurity to the local order-parameter field of the bulk, i.e., by a term $j_0 \int d\tau \vec{S}(\tau) \cdot \vec{\phi}(\vec{x}=0, \tau)$, but now the low-energy dynamics of $\phi(\vec{x}, \tau)$ will be represented in terms of spinon fields z introduced in Sec. II B.

A. Low-energy theory

It is easy to see that an appropriate choice of a linear combinations of the spinons defined in Eq. (4), namely

$$\begin{aligned} z'_\uparrow &= \frac{1}{\sqrt{2}} (z_\uparrow + iz_\downarrow), \\ z'_\downarrow &= \frac{1}{\sqrt{2}} (-iz'_\uparrow + z_\downarrow) \end{aligned} \quad (10)$$

enables us to write expression (4) in an alternative, but very convenient way:

$$\phi(\vec{x}=0) = \Re(\vec{n}_1 + i\vec{n}_2) = z'_\alpha \frac{\vec{\sigma}_{\alpha\beta}}{2} z'_\beta. \quad (11)$$

Note that this rotation leaves the bulk action invariant.

The appropriate model to describe a magnetic impurity in a topological spin liquid with a Z_2 gauge structure is thus

$$\begin{aligned} \mathcal{S} &= \frac{1}{g} \int d^d x d\tau (|\partial_x z_\sigma|^2 + |\partial_\tau z_\sigma|^2) \\ &+ \int d^d x d\tau \kappa(x, \tau) \left(\sum_\sigma |z_\sigma|^2 - 1 \right) \\ &+ j_0 \int d\tau \vec{S} \cdot z_\sigma^* \frac{\vec{\sigma}_{\sigma\sigma'}}{2} z_{\sigma'}(\vec{x}=0) \\ &+ \mathcal{S}_{\text{Berry}}[\vec{S}], \end{aligned} \quad (12)$$

and was proposed recently by us.²⁸

The most important feature of model (12) is that the impurity is coupled to a bilinear of the elementary bulk excitations (i.e., the spinons). This has to be contrasted to the impurity theory with collinear bulk ordering, where the impurity spin couples *linearly* to the magnetic (triplon) modes. The consequences of this difference will be examined below and turn out to be crucial for the fate of the impurity near the bulk critical point. Thus, apart from the strong constraint on the bulk spinons, the model (12) strongly resembles the *fermionic* Kondo model and constitutes its straightforward extension to a bosonic environment.

In the following, we concentrate on the impurity behavior at the bulk critical point, i.e., for gapless spinons. In the gapped case, weak impurity coupling will be irrelevant, and the impurity will decouple from the bulk in the low-energy limit. However, in analogy to fermionic Kondo models with a gapped density of states and broken particle-hole symmetry,¹⁴ a first-order quantum transition will take place upon increasing j_0 , beyond which a strong-coupling state is realized.

B. Weak-coupling RG analysis

A RG treatment of the action presented in Eq. (12) can be performed perturbatively in j_0 . In addition, the constraint $\sum_\sigma z_\sigma^* z_\sigma = 1$ is relaxed and treated on the mean-field level (this is equivalent to giving the spinons a mass shift). The influence of such bulk interaction terms will be considered in Sec. IV C. At zero temperature, the renormalized spinon mass vanishes at criticality, and the spinons become soft. This is the regime we focus on, and which is described by the simpler action:

$$\begin{aligned} \mathcal{S} &= \frac{1}{g} \int d^d x d\tau (|\partial_x z_\sigma|^2 + |\partial_\tau z_\sigma|^2) \\ &+ j_0 \int d\tau \vec{S} \cdot z_\sigma^* \frac{\vec{\sigma}_{\sigma\sigma'}}{2} z_{\sigma'}(\vec{x}=0) \\ &+ \mathcal{S}_{\text{Berry}}[\vec{S}]. \end{aligned} \quad (13)$$

In order to use diagrammatic methods it is convenient to represent the impurity spin in terms of Schwinger bosons (one could equally well choose to work with Abrikosov

fermions). Restricting ourselves to an impurity spin 1/2, we introduce thus bosonic operators b_σ which obey the following constraint

$$Q = \sum_\sigma b_\sigma^\dagger b_\sigma = 1. \quad (14)$$

This allows for a faithful impurity spin representation according to

$$\vec{S} = b_\sigma^\dagger \frac{\vec{\sigma}_{\sigma\sigma'}}{2} b_{\sigma'}. \quad (15)$$

In terms of these bosonic operators, we can formulate the full impurity action:⁴⁴

$$\begin{aligned} \mathcal{S} = & \frac{1}{g} \int d^d x d\tau z_\sigma^* (-\partial_x^2 - \partial_\tau^2) z_\sigma + \int d\tau \bar{b}_\sigma (\partial_\tau + \lambda) b_\sigma \\ & + j_0 \int d\tau \bar{b}_\sigma \frac{\vec{\sigma}_{\sigma\sigma'}}{2} b_{\sigma'} z_\alpha^* \frac{\vec{\sigma}_{\alpha\beta}}{2} z_\beta (\vec{x} = 0) \\ & + \frac{v_0}{4} \int d\tau z_\sigma^* z_\sigma (\vec{x} = 0), \end{aligned} \quad (16)$$

where we implement the constraint (14) exactly by taking the limit $\lambda \rightarrow \infty$.^{45,46}

In Eq. (16), we have included a potential scattering term v_0 on the impurity location $\vec{x} = 0$. In contrast to the fermionic case, such a term is generated perturbatively in the RG flow. This implies that for finite j , $v = 0$ cannot be a fixed point of the RG – this is intimately related to the bosonic nature of the bulk, as bosons cannot show particle–hole symmetry.

The RG treatment starts by determining the tree-level scaling dimensions of the couplings, yielding:

$$\dim[j_0] = \dim[v_0] = d - 2 \equiv \epsilon. \quad (17)$$

Both couplings are marginal in two dimensions; this allows for a controlled RG procedure, which we shall perform here using the standard field-theoretic scheme. Renormalized couplings are introduced as $j_0 = \frac{2}{gS_d} \mu^{-\epsilon} \frac{Z_j}{Z_b} j$ and $v_0 = \frac{2}{gS_d} \mu^{-\epsilon} \frac{Z_v}{Z_b} v$, where S_d denotes $S_d = \frac{2}{\Gamma(\frac{d}{2})(4\pi)^{d/2}}$. At two-loop order (see App. A) we find the following beta functions

$$\begin{aligned} \beta(j) &= \epsilon j + v j + \frac{j^3}{2} + \mathcal{O}(j^5), \\ \beta(v) &= \epsilon v + \frac{v^2}{2} + \frac{3}{2} j^2 + \mathcal{O}(j^4), \end{aligned} \quad (18)$$

where $\epsilon = d - 2$ for non-interacting bulk bosons. (This corrects a sign error in the result published in Ref. 28.) It is important to note that $\beta(j)$ [$\beta(v)$] does not contain even (odd) powers of j , respectively. This is the consequence of the invariance of the action (16) w.r.t. the transformation

$$j_0 \rightarrow -j_0 \quad \text{and} \quad z_\sigma \rightarrow \epsilon_{\sigma\sigma'} z_{\sigma'}^*, \quad (19)$$

which also implies that ferromagnetic and antiferromagnetic impurity coupling are equivalent. (Note again here

that the z are not canonical bosons – the corresponding operators simply commute.)

The solution of the two-loop flow equations is depicted in Fig. 1. The weak-coupling RG flow has four fixed points: the trivial (Gaussian) fixed point LM with $(v^*, j^*) = (0, 0)$; a potential scattering fixed point PS, given by $(v^*, j^*) = (-2\epsilon, 0)$; and a pair of critical fixed point, located at $(v^*, j^*) = (-\epsilon - \frac{\epsilon^2}{6}, \pm \frac{\epsilon}{\sqrt{3}})$ and denoted QCP.

Let us quickly discuss the physical implications of the present RG flow (but note that certain changes will arise from the consideration of bulk interactions, see below).

For $\epsilon > 0$ and $j \neq 0$, the flow indicates two stable phases, namely the local-moment phase (LM), and a strong-coupling phase at large $|j|$ (the Hamiltonian is symmetric under $j_0 \rightarrow -j_0$) and large negative v . The two phases are separated by a continuous quantum phase transition, controlled by QCP, with a correlation length exponent given by

$$\frac{1}{\nu} = |\epsilon| - \frac{\epsilon^2}{12} + \mathcal{O}(\epsilon^3), \quad (20)$$

characterizing the vanishing crossover energy scale near criticality. The pure potential scattering problem, $j = 0$, has two phases as well, which can be easily understood from the exact local spinon Green function:

$$G_0(i\nu) = \frac{G_0(i\nu)}{1 + (v_0/4)G_0(i\nu)} \quad (21)$$

$$\text{where } G_0(i\nu) = \int \frac{d^d k}{(2\pi)^d} \frac{g}{\nu^2 + k^2}. \quad (22)$$

Values $v > -2\epsilon$ flow to zero (the denominator in Eq. (21) is regular), whereas $v < -2\epsilon$ induces a bound state (a pole appears in the Green function of the bosons). The physical properties of LM are that of a decoupled impurity, i.e., susceptibility and entropy obey $\chi_{\text{imp}} = 1/(4T)$, $S_{\text{imp}} = \ln 2$ in the low-temperature limit. The strong-coupling regime cannot be analyzed using the present RG; a combination of large- N methods and strong-coupling models indicates that true screening can occur (for both signs of j_0), with a finite impurity susceptibility and vanishing entropy.²⁸ Finally, at the critical point (QCP) properties similar to Eq. (9) obtain.

For $\epsilon < 0$, the weak-coupling regime is unstable, and the flow generically is towards strong coupling – this can be related to the bare boson density of states, Eq. (22), diverging as $\nu \rightarrow 0$. Nevertheless, there is still a QCP, which separates the strong-coupling (screened) regime from a pure potential-scattering phase at positive v (controlled by a now stable PS fixed point).

For $\epsilon = 0$ no quantum phase transition occurs, and there is logarithmically slow flow to strong coupling (see below for corrections to this picture coming from bulk interactions).

Overall, the RG flow is strikingly different from an impurity which is coupled to gapless spin-1 bosons

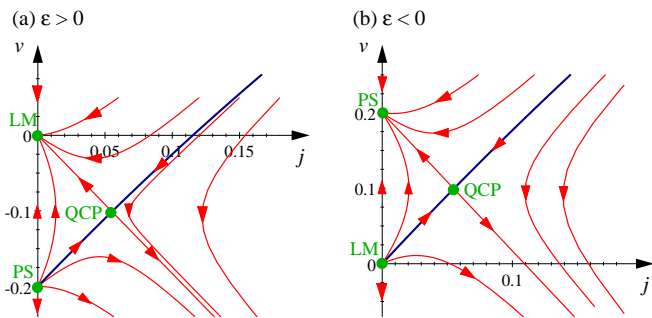


Figure 1: RG flow of the spinon Kondo model (16) at the bulk critical point. (a) $\epsilon > 0$; (b) $\epsilon < 0$. ($\epsilon = d - 2$ for non-interacting spinons; note that ϵ may be non-zero in $d = 2$ owing to bulk spinon interactions.) QCP denotes the boundary quantum critical point and the blue line is the separatrix, separating a strongly coupled phase from either a local moment (LM) regime or a potential scattering (PS) a zero Kondo coupling. The curves have been calculated from (18) for $\epsilon = \pm 0.1$. Note that the flow is symmetric w.r.t. $j \leftrightarrow -j$.

(Sec. III), where the coupling γ flows towards a *stable* intermediate-coupling fixed point.

C. The role of bulk interactions

Within the above weak-coupling RG the bulk interactions (represented by the constraint $\sum_{\sigma} |z_{\sigma}|^2 = 1$) were only treated at the mean-field level. Unfortunately, a consistent RG fully including the bulk interactions cannot be performed: the appropriate bulk non-linear sigma model is perturbatively accessible near $d = 1$ (while softening the bulk interaction allows an expansion in $3 - d$, see below), but expansions around both $d = 1$ and $d = 3$ are incompatible with the bare scaling dimension of the impurity coupling j_0 , which is marginal in $d = 2$. (This is in contrast to the situation in Sec. III where *both* bulk and boundary couplings were marginal at $d = 3$.)

The treatment of bulk interactions in the present spinon case is, however, physically important, both at weak coupling (to be discussed below) and at strong coupling – this was discussed in some detail in Ref. 28, but requires further work which is beyond the scope of this paper.

Let us qualitatively discuss the role of bulk spinon interactions at weak coupling. The scaling dimensions of j and v are determined by the local bulk spin correlations. In the interacting bulk theory, this decay is given as $\chi(\tau) \propto 1/\tau^{d-1+\eta}$ where η is the anomalous dimension. (Note that $\eta = 1$ for non-interacting spinons, whereas $\eta = 0$ in the case of a standard ϕ^4 theory controlled by a Gaussian fixed point.) This implies that $\dim[j_0] = \dim[v_0] = (d-3+\eta)/2$, i.e., the $\epsilon = d-2$ in the RG equations (18) should be replaced by $\epsilon = (d-3+\eta)/2$. The QCP in the incommensurate magnet has $\eta > 1$ in

$d = 2$ (for details see Refs. 32,33), i.e., a boundary quantum phase transition as shown in Fig. 1(a) is indeed possible for the physical two-dimensional case.

We note that this analysis (i.e. including η in the scaling dimensions of j and v) is in principle correct at one-loop order; at higher orders interference processes between bulk and boundary interactions can be expected. No systematic treatment of those is possible in the present formulation. Therefore, we propose a more rigorous way to incorporate bulk interactions, which leads us to a bosonic version of the Anderson impurity model.

1. Derivation of the bosonic Anderson model

Our goal is to find a representation of the model (16) which allows to perturbatively control both bulk and boundary interactions at the same time. To this end, we reformulate the impurity part, i.e., switch from a Kondo to an Anderson impurity model – such a scheme has proven extremely successful for the pseudogap Kondo model.⁷

Two transformations will convert the original model (16) into a new one, where bulk and boundary interactions have a common critical dimension: (a) an inverse Schrieffer-Wolff transformation (in analogy to the pseudogap Kondo case), which transforms the Kondo into an Anderson model and renders the hybridization between impurity and bulk marginal in $d = 3$; (b) replacing the hard constraint on the spinons by a “soft” self-interaction of the type $u_0(|z_{\sigma}|^2 - 1)^2$ – this term is marginal in $d = 3$ as well. (As will become clear, step (a) requires the existence of a strong-coupling singlet state with screening in the original model.) With steps (a) and (b) we are led to propose the following field theory:

$$\begin{aligned} \mathcal{S} = & \int d^d x d\tau \left[\frac{1}{g} (|\partial_x z_{\sigma}|^2 + |\partial_{\tau} z_{\sigma}|^2) + u_0 z_{\sigma}^* z_{\sigma} z_{\sigma}^* z_{\sigma} \right] \\ & + \int d\tau [\bar{b}_0 (\partial_{\tau} + \lambda + \epsilon_0) b_0 + \bar{b}_{\sigma} (\partial_{\tau} + \lambda) b_{\sigma}] \\ & + w_0 \int d\tau [\bar{b}_{\sigma} b_0 z_{\sigma} + \text{h.c.}] . \end{aligned} \quad (23)$$

We have left out a bulk mass term $\propto z_{\sigma}^2$, as we are interested in the bulk critical point. The impurity is now a three-level system (similar to an Anderson model with infinite repulsion), represented by three auxiliary particles b_{σ} ($\sigma = \uparrow, \downarrow$) and b_0 – note that b_0 may be interpreted as the empty impurity state. The impurity transition is tuned by the value of ϵ_0 : for $\epsilon_0 > 0$ the impurity is in a doublet state (i.e. unscreened) whereas for $\epsilon_0 < 0$ the state is a singlet (these statements apply for $w_0 \rightarrow 0$, finite w_0 will shift the impurity critical point). The Hilbert space dimension is enforced by the constraint $Q = \sum_{\sigma} b_{\sigma}^{\dagger} b_{\sigma} + b_0^{\dagger} b_0 = 1$. Technically, this is again implemented via a chemical potential $\lambda \rightarrow \infty$.^{45,46}

The action (23) incorporates three main ingredients: (i) it contains an interaction term u_0 in the bulk, which is marginal in $d = 3$; (ii) the hybridization w_0 is marginal in $d = 3$ as well; (iii) in the ‘‘Kondo’’ limit, i.e., for a large positive singlet energy ϵ_0 , a Schrieffer-Wolff transformation allows to integrate out the b_0 field, and leads to the previous bosonic Kondo interaction (16). The model (23) at $d = 3$ is thus strongly reminiscent of the pseudogap Anderson impurity model (with infinite impurity Coulomb energy) and linear density of states.⁸ (Another bosonic Anderson model was recently introduced by Lee and Bulla,⁴⁷ which, however, displays different physics, as the model of Ref. 47 is spinless, but with finite on-site repulsion.)

We will proceed with deriving the RG flow for the Anderson model (23).

2. RG analysis of the bosonic Anderson model

The RG flow for both the bulk and impurity interactions, u_0 and w_0 , can be perturbatively controlled in $\epsilon = \frac{3-d}{2}$. This allows a consistent calculation of the critical properties of the fully interacting bosonic impurity model. The details of this calculation are presented in App. B.

We introduce renormalized couplings according to $w_0 = \mu^\epsilon \sqrt{\frac{2}{gS_d}} \frac{Z_w}{\sqrt{Z_{b_0} Z_{b_\sigma} Z_z}} w$ and $u_0 = \mu^{2\epsilon} \frac{4}{S_d g^2} \frac{Z_u}{Z_z^2} u$. Placing ourselves at both the bulk and boundary critical points (!), we find the following flow equations to one-loop order:

$$\begin{aligned}\beta(w) &= \epsilon w - \frac{3}{2} w^3, \\ \beta(u) &= 2\epsilon u - 12u^2.\end{aligned}\quad (24)$$

These RG equations describe the non-trivial flow of both bulk and boundary interactions at the critical point in $d < 3$. Higher-order contributions (not shown here) contain the above-mentioned interference processes and induce a feedback of the bulk interaction u into the impurity flow.

We refrain from a more detailed analysis at this point: qualitatively, the RG approaches in Secs. IV B and IV C 2 yield similar results; a quantitative comparison is difficult as the two expansions are around a lower critical and upper critical dimension of the impurity problem, respectively. Let us, however, emphasize that we have demonstrated how a systematic expansion, analogous to the one in Ref. 18 for impurity models in collinear magnets (i.e. treating bulk and boundary interactions on equal footing) can be set up in the non-collinear case as well.

V. A MAGNETIC IMPURITY IN A TWO-COMPONENT CANONICAL BOSE GAS

In this last part, we briefly introduce and analyze the problem of a two-state system³⁰ (described by a magnetic pseudospin impurity) coupled to a two-component non-relativistic Bose gas.³¹ This extends the kind of bosonic impurity models, introduced above in the context of quantum antiferromagnets, to the field of cold atomic gases.

A. The model

Technically, the main difference to the situation in the previous section is that the bulk now consists of *canonical* bosons. The action assumes the form:

$$\begin{aligned}\mathcal{S} &= \int d^d x d\tau \bar{a}_\sigma(x, \tau) (\partial_\tau - \partial_x^2 + m) a_\sigma \\ &+ j_0 \int d\tau \vec{S} \cdot \bar{a}_\sigma \frac{\vec{\sigma}_{\sigma\sigma'}}{2} a_{\sigma'}(\vec{x} = 0) \\ &+ \frac{v_0}{4} \int d\tau \bar{a}_\sigma a_\sigma(\vec{x} = 0) \\ &+ \mathcal{S}_{\text{Berry}}[\vec{S}],\end{aligned}\quad (25)$$

where we consider canonical bosonic particles, a_σ , with two internal degrees of freedom ($\sigma = \uparrow, \downarrow$ here) and a mass m (i.e., chemical potential). In the field of ultracold trapped gases, usually performed with fixed particle number, $m \rightarrow 0$ in the low-temperature limit. Interactions among bulk bosons are neglected; to lowest order, they lead to a temperature-dependent renormalization of m . The impurity couples to the bosonic spin density at site $\vec{x} = 0$ with a Kondo-type exchange interaction, but an Anderson-like Hamiltonian similar to Eq. (23) could be considered as well.

B. Weak-coupling analysis

In contrast to spinon-based models, we realize that there is no invariance under the transformation $j_0 \rightarrow -j_0$, i.e., ferromagnetic and antiferromagnetic impurity coupling are no longer equivalent. However, as in the spinon case, a potential scattering term is generated during the flow even for $v_0 = 0$.

In the remainder, we focus on the weak-coupling analysis in the massless case, $m = 0$. (In the massive case, $m > 0$ at $T = 0$, we again expect a first-order transition as function of j_0 .) A tree-level dimensional analysis yields

$$\dim[j_0] = \dim[v_0] = d - 2 \equiv \epsilon, \quad (26)$$

similar to the model in Sec. IV B. We thus introduce dimensionless couplings according to $j_0 = \mu^{-\epsilon} \frac{1}{S_d} \frac{Z_w}{Z_b} j$ and

$v_0 = \mu^{-\epsilon} \frac{1}{S_d} \frac{Z_v}{Z_b} v$ and find to one-loop order

$$\begin{aligned}\beta(j) &= \epsilon j - \frac{j^2}{2} + \frac{v j}{2}, \\ \beta(v) &= \epsilon v + \frac{v^2}{4} + \frac{3}{4} j^2.\end{aligned}\quad (27)$$

Remarkably, this result is exact to *all* orders in perturbation theory (this was previously shown for non-relativistic ϕ^4 -theory with local interactions^{1,48}). Technically, the reason for that lies in the diagrammatic structure of the problem, where only ladder-like diagrams can be different from zero in the limit $T = 0$. Higher-order terms are cancelled by the appropriate counterterms. Physically, the exactness of Eq.(27) is tied to the fact that the expansion is performed around a trivial vacuum state.

The RG flow, derived from Eq. (27), is depicted in Fig. 2. For positive (antiferromagnetic) j , it is qualitatively similar to the one of the spinon model in Sec. IV B. From Eq. (27) one finds four fixed points: the local-moment (LM) fixed point at $(v^*, j^*) = (0, 0)$, a potential-scattering (PS) fixed point at $(v^*, j^*) = (-4\epsilon, 0)$, and two critical fixed points at $(v^*, j^*) = (-\epsilon, \epsilon)$ and $(v^*, j^*) = (-3\epsilon, -\epsilon)$. For both QCP, the correlation length exponent is

$$\frac{1}{\nu} = |\epsilon|, \quad (28)$$

which again is exact to all orders in perturbation theory.

The structure of the phase diagram for both positive and negative ϵ is thus similar to the spinon case in Sec. IV B. However, ferromagnetic and antiferromagnetic j_0 are no longer equivalent, suggesting the existence of two distinct strong-coupling phases for $j < 0$ and $j > 0$ (where true screening is likely to occur only in the latter case).

For $\epsilon = 0$ and $j > 0$, logarithmic flow to strong coupling occurs, with a screening temperature given by $\ln T^* \propto -1/j_0$ as in the conventional Kondo problem.

Thus, the situation of a two-level impurity coupled to a two-component Bose gas, with a pseudospin–pseudospin coupling, allows for three distinct phases (given $j_0 \neq 0$): a weakly coupled (unscreened) phase and two strong-coupling phases. The present analysis can be easily generalized to an arbitrary number of pseudospin components or larger effective spin sizes; at weak coupling no qualitative changes are expected. However, the precise nature of the ground state at strong coupling depends on microscopic parameters of the Bose gas, such as spin size and the value of the repulsion between bosonic atoms.²⁸ More elaborate strong-coupling methods are required to address this issue.

Last not least, let us point out another remarkable feature of the above model (25): its RG flow is equivalent to a fermionic Kondo problem with full band asymmetry, i.e. with a chemical potential tuned to the band edge. This was considered previously,⁴⁹ and we comment on this point in App. C.

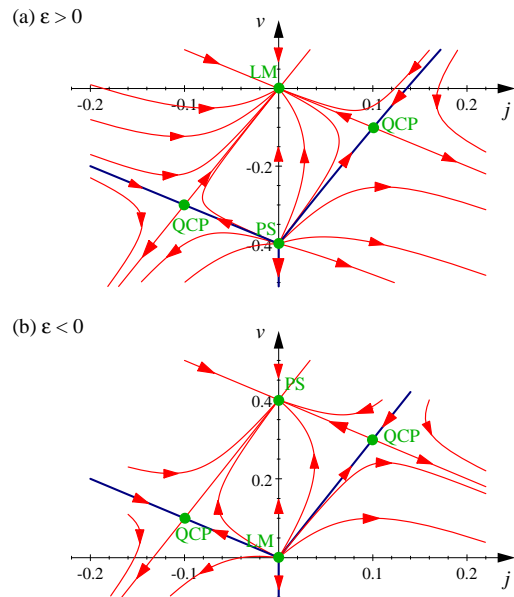


Figure 2: RG flow of the Kondo model with massless canonical bosons, Eq. (25). (a) $\epsilon > 0$; (b) $\epsilon < 0$. ($\epsilon = d - 2$ for non-interacting bosons; again, ϵ may be non-zero in $d = 2$ due to bulk interactions.) The curves have been calculated from (27) for $\epsilon = \pm 0.1$.

VI. CONCLUSION

In this paper, we have introduced a new class of quantum impurity models, describing the dynamics of a two-level system (spin) coupled to an external bosonic spin-carrying environment. Two different situations have been studied in the weak-coupling regime, namely a spin 1/2 magnetic impurity in a class of Z_2 spin liquids, and a local defect in a two-component Bose gas.

For massless bulk particles, we have derived the renormalization group flow of the impurity coupling constants. While some differences in the RG flow appear between the above two realizations, the following generic features appear: (I) an impurity quantum phase transition is possible which separates a local-moment regime (decoupled impurity) from a strongly coupled impurity; (II) in contrast to a magnetic impurity coupled to a collinear bulk magnet described by a standard ϕ^4 theory, there is no stable intermediate-coupling fixed point, but instead runaway flow to strong coupling. (For gapped bulk particles, a first-order transition will generically appear, in analogy to gapped fermionic Kondo models.) At strong coupling, the nature of the ground state depends on microscopic details (and was not investigated further here), but quenching of the impurity entropy may obtain.²⁸

In summary, our results underline that the dynamics of impurity degrees of freedom depends crucially on the nature of the elementary excitations of the surrounding environment. Hence, impurity properties may be

used as probes for exotic bulk excitations. On the experimental side, Cs_2CuCl_4 has been proposed to be a realization of a spin-1/2 frustrated antiferromagnet on an anisotropic triangular lattice, which possibly features spinon excitations.^{50,51} Studying the physics of dilute magnetic impurities in this material, e.g. the temperature dependence of NMR Knight shifts or of the impurity contribution to the susceptibility, will clearly help to resolve the nature of the bulk magnetic state.

Acknowledgments

We thank S. Sachdev, T. Senthil and G. Zaránd for valuable discussions, and K. Damle for a collaboration at the early stage of this work. Furthermore, we would like to acknowledge the creators of Jaxodraw⁵², which simplified the drawing of the Feynman diagrams significantly. This research was supported by the DFG through the Center for Functional Nanostructures (Karlsruhe) and SFB 608 (Köln), as well as through the Virtual Quantum Phase Transitions Institute in Karlsruhe.

Appendix A: WEAK-COUPLING RG FOR THE BOSONIC KONDO MODEL

In this appendix we derive the RG equations for the bosonic Kondo model with bulk spinons (the derivation is kept in a form which is also appropriate to treat the case of canonical bosons as well as electrons; the only occurring modifications manifest themselves in the values of the corresponding Feynman diagrams). The RG equations of bosons are very different from those of electrons, which is the reason why we present a rather detailed analysis. The crucial difference resides in the fact that during the renormalization process a potential scattering term is generated. In order to properly deal with this complication we start with a generalized version of the model proposed in Eq. (12) which allows for fully spin-anisotropic couplings. This enables us to deal with the Kondo interaction and the potential scattering term at a time without worrying about newly generated terms.

The action we analyze has the following very general form

$$\begin{aligned}
\mathcal{S} = & \frac{1}{g} \int d^d x d\tau \sum_{\sigma} z_{\sigma}^* (-\partial_{\tau}^2 - \partial_x^2) z_{\sigma} \\
& + \sum_{\sigma} \int d\tau \bar{b}_{\sigma} (\partial_{\tau} + \lambda) b_{\sigma} \\
& + \alpha_0 \int d\tau \sum_{\sigma \neq \sigma'} z_{\sigma}^* z_{\sigma'} \bar{b}_{\sigma'} b_{\sigma} \\
& + \beta_0 \int d\tau \sum_{\sigma} z_{\sigma}^* z_{\sigma} \bar{b}_{\sigma} b_{\sigma} \\
& + \gamma_0 \int d\tau \sum_{\sigma \neq \sigma'} z_{\sigma}^* z_{\sigma} \bar{b}_{\sigma'} b_{\sigma'} . \tag{A1}
\end{aligned}$$

a. Weak-coupling RG procedure

The tree-level scaling dimensions of the general couplings constants are

$$\dim[\alpha_0] = \dim[\beta_0] = \dim[\gamma_0] = d - 2 = \epsilon . \tag{A2}$$

Based on this analysis we introduce dimensionless couplings according to

$$\begin{aligned}
\alpha_0 &= \mu^{-\epsilon} \frac{2}{g S_d} \frac{Z_{\alpha}}{Z_b} \alpha , \\
\beta_0 &= \mu^{-\epsilon} \frac{2}{g S_d} \frac{Z_{\beta}}{Z_b} \beta , \\
\gamma_0 &= \mu^{-\epsilon} \frac{2}{g S_d} \frac{Z_{\gamma}}{Z_b} \gamma , \tag{A3}
\end{aligned}$$

where μ denotes an arbitrary but fixed energy scale (the renormalization scale) and $S_d = \frac{\Omega_d}{(2\pi)^d}$, where $\Omega_d = \frac{2\pi^{d/2}}{\Gamma(d/2)}$ with $\Gamma(x)$ being the Euler function. We furthermore state that during the course of renormalization the Schwinger boson field parametrizing the spin is renormalized according to

$$b_R = Z_b^{-1} b . \tag{A4}$$

We do not have to introduce renormalized fields for the bulk degrees of freedom since the influence of a single impurity on the bulk is an effect of the order $\mathcal{O}(1/N)$, which does not renormalize bulk degrees of freedom. The prefactor $\frac{2}{g S_d}$ can trivially be taken care of by rescaling the fields in Eq. (12) according to

$$z_{\sigma} = \sqrt{\frac{g S_d}{2}} z'_{\sigma} \tag{A5}$$

which has the only advantage of getting rid of bothersome factors in the course of the calculation. The generalized renormalized action (with appropriate counter-

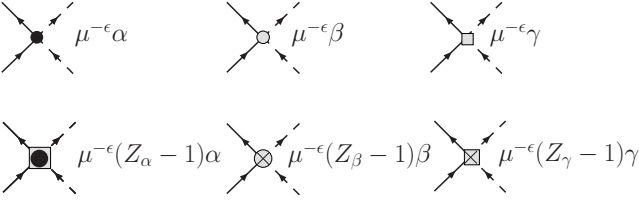


Figure 3: Graphical representation of all the occurring vertices; α is denoted as a black circle, its counterterm is represented by a big black circle in a box; the small grey dot and the big grey dot with a cross represent β and its counterterm; the small (big) grey box (grey box with a cross) represents γ (the counterterm of γ).

erms) reads:

$$\begin{aligned}
\mathcal{S}_R = & \frac{S_d}{2} \int d^d x d\tau \sum_{\sigma} z_{\sigma}^* (-\partial_{\tau}^2 - \partial_x^2) z_{\sigma} \\
& + \mu^{-\epsilon} \alpha \int d\tau \sum_{\sigma \neq \sigma'} z_{0,\sigma}^* z_{0,\sigma'} \bar{b}_{\sigma'} b_{\sigma} \\
& + \mu^{-\epsilon} \beta \int d\tau \sum_{\sigma} z_{0,\sigma}^* z_{0,\sigma} \bar{b}_{\sigma} b_{\sigma} \\
& + \mu^{-\epsilon} \gamma \int d\tau \sum_{\sigma \neq \sigma'} z_{0,\sigma}^* z_{0,\sigma} \bar{b}_{\sigma'} b_{\sigma'} \\
& + \int d\tau \sum_{\sigma} \bar{b}_{\sigma} (\partial_{\tau} + \lambda) b_{\sigma} + \sum_{\sigma} \int d\tau (Z_b - 1) \bar{b}_{\sigma} \partial_{\tau} b_{\sigma} \\
& + \mu^{-\epsilon} \alpha (Z_{\alpha} - 1) \int d\tau \sum_{\sigma \neq \sigma'} z_{0,\sigma}^* z_{0,\sigma'} \bar{b}_{\sigma'} b_{\sigma} \\
& + \mu^{-\epsilon} \beta (Z_{\beta} - 1) \int d\tau \sum_{\sigma} z_{0,\sigma}^* z_{0,\sigma} \bar{b}_{\sigma} b_{\sigma} \\
& + \mu^{-\epsilon} \gamma (Z_{\gamma} - 1) \int d\tau \sum_{\sigma \neq \sigma'} z_{0,\sigma}^* z_{0,\sigma} \bar{b}_{\sigma'} b_{\sigma'} .
\end{aligned} \tag{A6}$$

This is the appropriate starting point to iteratively construct the counterterms by demanding the action to be finite at a certain arbitrary but fixed renormalization point. The graphical representation of the vertices and the counterterms is shown in Fig. 3. The vertex α is denoted as a small black dot whereas the associated counterterm $(Z_{\alpha} - 1)\alpha$ is represented as a big black dot in a box. The interaction vertex β and its counterterm $(Z_{\beta} - 1)\beta$ are represented as a small grey dot and a big grey dot with a cross in the interior, whereas γ and the associated counterterm $(Z_{\gamma} - 1)\gamma$ are graphically represented as small grey box and a big grey box with a cross inside, respectively. In the diagrammatic expansion this enforces us to consider 6 interaction vertices for a consistent treatment.

The next step is to specify the renormalization conditions which will give the theory a finite limit once the

cutoff is sent to infinity according to

$$\begin{aligned}
\Gamma_b^2(i\nu - \lambda = i\bar{\nu} = 0) &= 0 , \\
\left. \frac{\partial}{\partial i\bar{\nu}} \Gamma_b^2(i\bar{\nu}) \right|_{i\bar{\nu}=\mu} &= 1 , \\
\left. \Gamma_{ss'ss'}^4 \right|_R &= \mu^{-\epsilon} \alpha , \\
\left. \Gamma_{ssss}^4 \right|_R &= \mu^{-\epsilon} \beta , \\
\left. \Gamma_{sss's'}^4 \right|_R &= \mu^{-\epsilon} \gamma ,
\end{aligned} \tag{A7}$$

where the subscript denotes the appropriate renormalization point, which we do not specify here. The first line fixes the impurity propagator, whereas the second line fixes the vertex functions. We once again stress the fact that the bulk properties will not receive singular corrections in any order of perturbation theory.

b. Result to one-loop order

To lowest loop order we can concentrate on the renormalization of the vertex functions since there is no propagator renormalization at one loop level (they will play a role at two loop level). To lowest loop order there are no propagator renormalizations. We choose a graphical representation of the renormalization conditions fixed in Eq. (A7). The renormalization conditions for the vertex functions are shown in Fig. 4, Fig. 5, and Fig. 6. Structurally there are only two types of diagrams occurring, whose most divergent part in an expansion in $1/\epsilon$ yields

$$\mu^{2\epsilon} \int_0^{\infty} dx \frac{x^{\epsilon+1}}{x(1+x)} = -\mu^{2\epsilon} \left(\frac{1}{\epsilon} + \mathcal{O}(\epsilon^0) \right) . \tag{A8}$$

By dressing the integral values with the appropriate interaction vertices we can determine the Z factors to lowest order as

$$\begin{aligned}
Z_{\alpha}^1 &= -(2\beta + 2\gamma) \frac{1}{\epsilon} , \\
Z_{\beta}^1 &= -\left(\frac{\alpha^2}{\beta} + 2\beta \right) \frac{1}{\epsilon} , \\
Z_{\gamma}^1 &= -\left(\frac{\alpha^2}{\gamma} + 2\gamma \right) \frac{1}{\epsilon} .
\end{aligned} \tag{A9}$$

c. Result to two-loop order

In order to derive the Z factors to two-loop order we only calculate the numerical values of the topologically distinct diagrams shown in Fig. 7. The actual vertex corrections are obtained by properly dressing the numerical

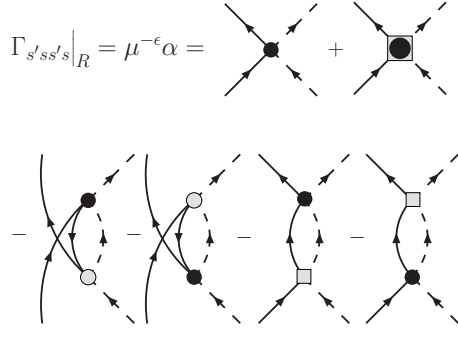


Figure 4: Graphical representation of the renormalization condition shown in Eq. (A7) determining the one-loop counterterm $(Z_\alpha - 1)^{(1)}$ (big black dot in box).

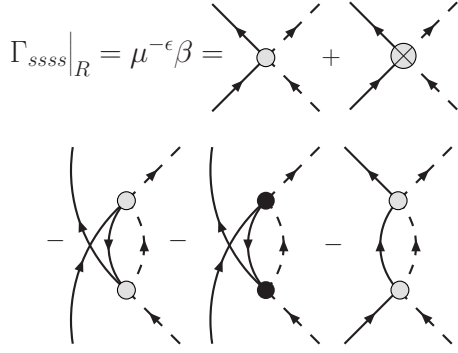


Figure 5: Graphical representation of the renormalization condition shown in Eq. (A7) determining the one-loop counterterm $(Z_\beta - 1)^{(1)}$ (big grey dot with a cross).

value of the integrals with the corresponding interaction vertices. All possible diagrams contributing to the two-loop renormalization factors are shown in Figs. 7 and 8. The diagrams contributing to Z_γ are not shown explicitly, since they can be obtained from the diagrams contribut-

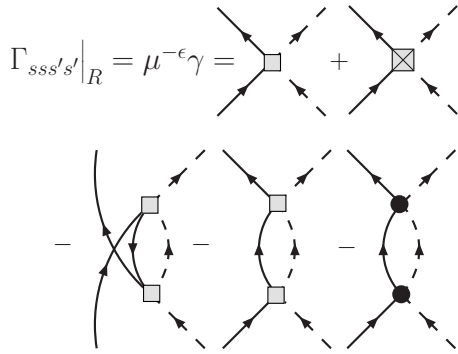


Figure 6: Graphical representation of the renormalization condition shown in Eq. (A7) determining the one-loop counterterm $(Z_\gamma - 1)^{(1)}$ (big grey box with a cross).

ing to Z_β by replacing grey dots by grey boxes. We start with the trivial diagrams (a) and (b) which are just the squares of the one-loop diagrams

$$(a) = (b) = \mu^{2\epsilon} \left(\frac{1}{\epsilon^2} + \mathcal{O}(\epsilon^0) \right). \quad (\text{A10})$$

The diagrams (c)...(j) are given by

$$(c\dots j) = \mu^{2\epsilon} \int_0^\infty dx \frac{x^\epsilon (x+2)^\epsilon}{1+x} \int_0^\infty dy \frac{y^\epsilon}{1+y}, \quad (\text{A11})$$

which to leading order yields

$$(c\dots j) = \mu^{2\epsilon} \left(\frac{1}{2\epsilon^2} + \mathcal{O}(\epsilon^0) \right). \quad (\text{A12})$$

The remaining diagram (k) evaluates to

$$\begin{aligned} (k) &= \mu^{2\epsilon} \int_0^\infty dx dy \frac{x^\epsilon y^\epsilon}{(x+y+1)(x+y)} \\ &= -\mu^{2\epsilon} \left(\frac{1}{2\epsilon} + \mathcal{O}(\epsilon^0) \right). \end{aligned} \quad (\text{A13})$$

We will re-encounter the same integral within the calculation of the field renormalization factor. In order to arrive at the final two loop Z -factors we dress the integral values with the appropriate interaction vertices. After some calculation we find

$$\begin{aligned} Z_\alpha &= 1 - \frac{2}{\epsilon} \left(\beta + \gamma - \frac{\beta\gamma}{2} \right) \\ &\quad + \frac{2}{\epsilon^2} \left(\alpha^2 + 2(\beta^2 + \beta\gamma + \gamma^2) \right), \\ Z_\beta &= 1 - \frac{2}{\epsilon} \left(\frac{\alpha^2}{2\beta} + \beta - \frac{\beta^2}{4} - \frac{\alpha^2\gamma}{4\beta} - \frac{\gamma^2}{4} \right) \\ &\quad + \frac{2}{\epsilon^2} \left(2(\beta^2 + \alpha^2) + \frac{\alpha^2\gamma}{\beta} \right), \\ Z_\gamma &= 1 - \frac{2}{\epsilon} \left(\frac{\alpha^2}{2\gamma} + \gamma - \frac{\gamma^2}{4} - \frac{\alpha^2\beta}{4\gamma} - \frac{\beta^2}{4} \right) \\ &\quad + \frac{2}{\epsilon^2} \left(2(\gamma^2 + \alpha^2) + \frac{\alpha^2\beta}{\gamma} \right). \end{aligned} \quad (\text{A14})$$

The next step consists of the propagator renormalization, whose recursion relation is shown in Fig. 9. We calculate the diagram shown in Fig. 9 (a). The dependence on the external frequency can be extracted by calculating

$$\begin{aligned} &\Sigma(i\nu_n - \lambda) - \Sigma(0) \\ &= (i\nu_n - \lambda) \mu^{2\epsilon} \int_0^\infty dx dy \frac{x^\epsilon y^\epsilon}{(x+y+1)(x+y)} \\ &= -(i\nu_n - \lambda) \mu^{2\epsilon} \left(\frac{1}{2\epsilon} + \mathcal{O}(\epsilon^0) \right). \end{aligned} \quad (\text{A15})$$

If we dress this integral with the appropriate vertices and apply the renormalization condition shown in Fig. 9 (note that $i\bar{\nu}_n = i\nu_n - \lambda$) we find

$$Z_b = 1 + \frac{1}{2\epsilon} (\alpha^2 + \beta^2 + \gamma^2). \quad (\text{A16})$$

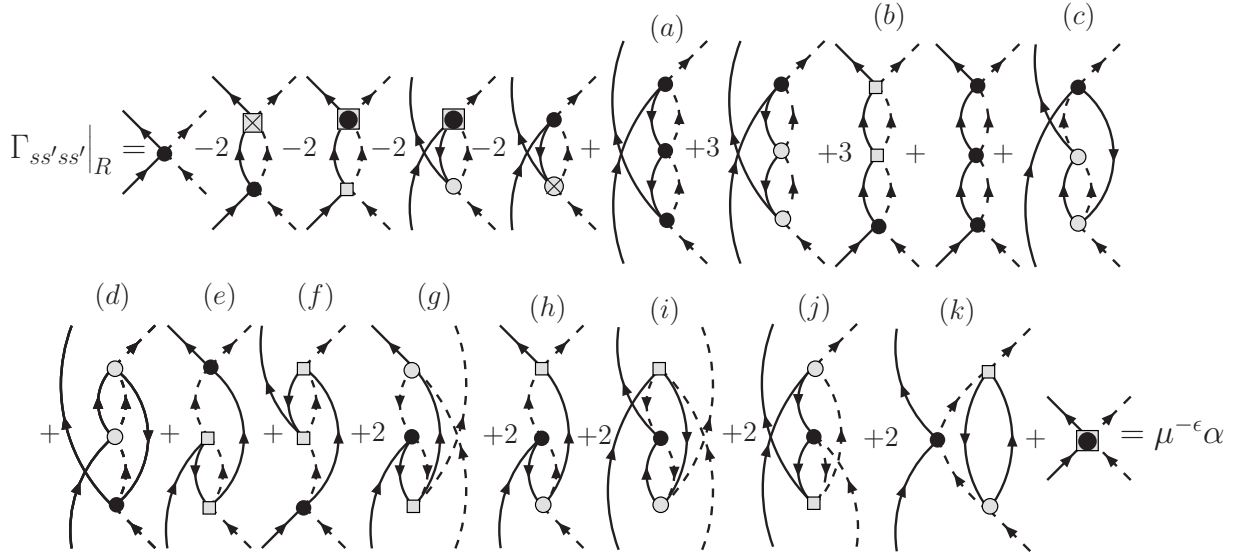


Figure 7: Graphical recursion relation for the two-loop contribution to the renormalization factor $(Z_\alpha - 1)^{(2)}$ (last term). Note that the counterterms appearing as internal vertices in the diagrams take their one-loop values $(Z_\alpha - 1)^{(1)}\alpha$, $(Z_\beta - 1)^{(1)}\beta$, $(Z_\gamma - 1)^{(1)}\gamma$. (a)-(k) denote topologically distinct diagrams.

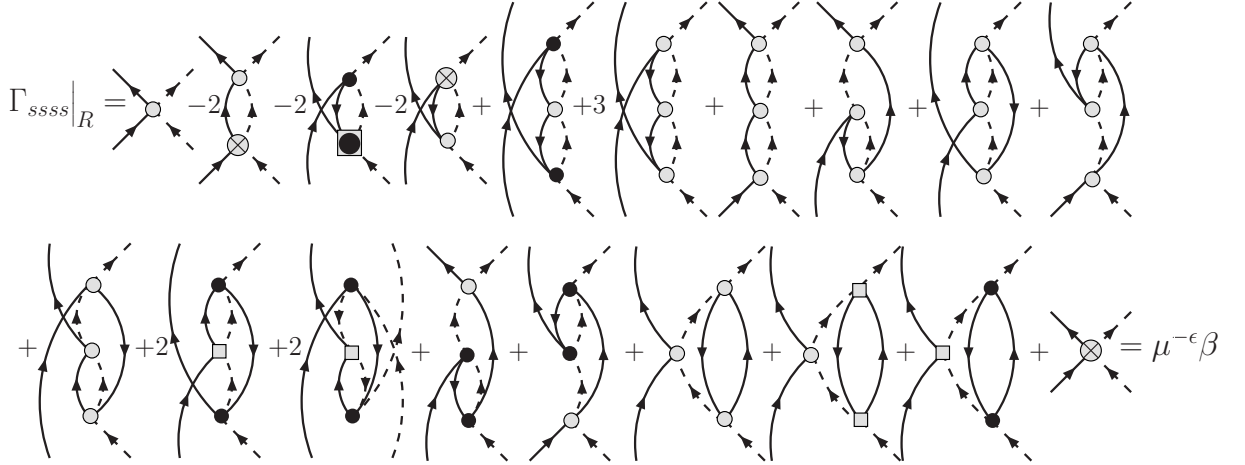


Figure 8: Graphical recursion relation for the two-loop contribution to the renormalization factor $(Z_\beta - 1)^{(2)}$ (last term). Note that the counterterms appearing as internal vertices in the diagrams take their one-loop values $(Z_\alpha - 1)^{(1)}\alpha$, $(Z_\beta - 1)^{(1)}\beta$, $(Z_\gamma - 1)^{(1)}\gamma$.

$$\frac{\partial}{\partial \bar{v}} \left[\text{a) } \text{b) } \text{c) } \right] \Big|_{i\bar{v}=\mu} - \oplus = 0$$

Figure 9: Recursion relation for the impurity field renormalization factor $(Z_b - 1)$ (crossed dot).

In order to derive the RG beta functions we use the fact that the bare couplings have no knowledge about the renormalization condition, which can be expressed as

$$\mu \frac{d\alpha_0}{d\mu} = \mu \frac{d\beta_0}{d\mu} = \mu \frac{d\gamma_0}{d\mu} = 0. \quad (\text{A17})$$

This leads to a set of coupled equations

$$\begin{aligned}
& - \epsilon\alpha + \alpha \frac{\partial \ln \left(\frac{Z_\alpha}{Z_f} \right)}{\partial \alpha} \beta(\alpha) + \alpha \frac{\partial \ln \left(\frac{Z_\alpha}{Z_f} \right)}{\partial \beta} \beta(\beta) + \alpha \frac{\partial \ln \left(\frac{Z_\alpha}{Z_f} \right)}{\partial \gamma} \beta(\gamma) = 0, \\
& - \epsilon\beta + \beta \frac{\partial \ln \left(\frac{Z_\beta}{Z_f} \right)}{\partial \alpha} \beta(\alpha) + \beta \frac{\partial \ln \left(\frac{Z_\beta}{Z_f} \right)}{\partial \beta} \beta(\beta) + \beta \frac{\partial \ln \left(\frac{Z_\beta}{Z_f} \right)}{\partial \gamma} \beta(\gamma) = 0, \\
& - \epsilon\gamma + \gamma \frac{\partial \ln \left(\frac{Z_\gamma}{Z_f} \right)}{\partial \alpha} \beta(\alpha) + \gamma \frac{\partial \ln \left(\frac{Z_\gamma}{Z_f} \right)}{\partial \beta} \beta(\beta) + \gamma \frac{\partial \ln \left(\frac{Z_\gamma}{Z_f} \right)}{\partial \gamma} \beta(\gamma) = 0,
\end{aligned} \tag{A18}$$

where the introduced β functions correspond to $\beta(\alpha) = \mu \frac{d}{d\mu} \alpha$ etc. These coupled equations can be solved iteratively, leading to

$$\begin{aligned}
\beta(\alpha) &= \epsilon\alpha + \alpha \left(\alpha^2 + (\beta - \gamma)^2 \right) + 2\alpha(\beta + \gamma), \\
\beta(\beta) &= \epsilon\beta + 2\beta \left(\frac{\alpha^2}{2\beta} + \beta \right) + \beta \left(\alpha^2 - \frac{\alpha^2\gamma}{\beta} \right), \\
\beta(\gamma) &= \epsilon\gamma + (\alpha^2 + 2\gamma^2) - \alpha^2(\beta - \gamma).
\end{aligned} \tag{A19}$$

In order to arrive at the actual bosonic Kondo model (Eq. (12)) with potential scattering we have to make the following identifications

$$\alpha = \frac{j_\perp}{2}, \quad \beta = \frac{j_z}{4} + \frac{v}{4}, \quad \text{and} \quad \gamma = -\frac{j_z}{4} + \frac{v}{4}. \tag{A20}$$

The flow equations of the physical couplings j_\perp, j_z, v are related to the intermediate quantities α, β, γ according to

$$\begin{aligned}
\beta(j_\perp) &= 2\beta(\alpha), \\
\beta(j_z) &= 2[\beta(\beta) - \beta(\gamma)], \\
\beta(v) &= 2[\beta(\beta) + \beta(\gamma)],
\end{aligned} \tag{A21}$$

with the interaction parameters chosen as shown in Eq. (A20). This leads to the following flow equations

$$\begin{aligned}
\beta(j_\perp) &= \epsilon j_\perp + v j_\perp + \frac{j_\perp j_z^2}{4} + \frac{j_\perp^3}{4}, \\
\beta(j_z) &= \epsilon j_z + v j_z + \frac{j_\perp^2 j_z}{4}, \\
\beta(v) &= \epsilon v + \frac{v^2}{2} + j_\perp^2 + \frac{j_z^2}{2},
\end{aligned} \tag{A22}$$

or in the spin-isotropic situation

$$\begin{aligned}
\beta(j) &= \epsilon j + v j + \frac{j^3}{2}, \\
\beta(v) &= \epsilon v + \frac{v^2}{2} + \frac{3}{2} j^2
\end{aligned} \tag{A23}$$

which are the RG equations (18) quoted in the main text.

The RG equations for the model of canonical bosons, Eq. (27) in Sec. V, are obtained from the same diagrammatic expansion (albeit with different numerical values

for the diagrams). The observation that the RG equations are exact to *all* orders comes can be easily understood by noting that the counterterms cancel all higher-order contributions because the only non-vanishing diagrams are ladder-like (in electronic language one would call these diagrams the Cooper diagrams), see Ref. 1.

Appendix B: RG FOR THE BOSONIC ANDERSON MODEL

Within this section we derive the RG equations for the bosonic version of the infinite- U Anderson model of Sec. IV C 1. After a Fourier transformation for the quadratic bulk part, the action of the model (23) reads

$$\begin{aligned}
\mathcal{S} &= \frac{1}{g} \beta^{-1} \sum_{\nu_n, \sigma} \int \frac{d^d k}{(2\pi)^d} z_\sigma^*(\nu_n, k) [\nu_n^2 + k^2] z_\sigma(\nu_n, k) \\
&+ u_0 \int d^d x d\tau z_\sigma^* z_\sigma z_{\sigma'}^* z_{\sigma'} \\
&+ \int d\tau \bar{b}_0 (\partial_\tau + \lambda) b_0 + \int d\tau \bar{b}_\sigma (\partial_\tau + \lambda) b_\sigma \\
&+ w_0 \int d\tau [\bar{b}_\sigma b_0 z_\sigma(\tau) + \text{h.c.}].
\end{aligned} \tag{B1}$$

The flow equations for the bulk interaction u_0 and the hybridization w_0 will not mix to one-loop order. In the following we will ignore the renormalization of the mass difference between the different impurity levels [ϵ_0 in (23)], i.e., we work at criticality. We introduce renormalized couplings according to

$$\begin{aligned}
w_0 &= \mu^\epsilon \sqrt{\frac{2}{g S_d}} \frac{Z_w}{\sqrt{Z_{b_0} Z_{b_\sigma} Z_z}} w \quad \text{and} \\
u_0 &= \mu^{2\epsilon} \frac{4}{S_d g^2} \frac{Z_u}{Z_z^2} u,
\end{aligned} \tag{B2}$$

where $\epsilon = \frac{3-d}{2}$. It is interesting to note that technically we have a version of the RG of a model which is at its upper critical dimension (both for the bulk and the impurity), whereas the RG for the bosonic Kondo model is reminiscent of an RG at the lower critical dimension. The vertices of the theory are shown in Fig. 10.

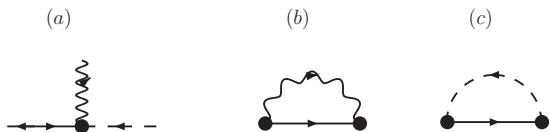


Figure 10: (a) Interaction vertex between bulk and impurity in the bosonic Anderson model; the wiggly line denotes the particle b_0 , the dashed line is b_σ and the full line stands for z_σ (incoming arrow) or z_σ^* (outgoing arrow). (b) and (c) denote self-energy corrections to the local levels b_σ (b) and b_0 (c).

The calculation for the renormalization of the hybridization w completely parallels the analysis in the pseudogap infinite- U Anderson model, which was presented in Ref. 7, and therefore without showing further calculational details leads to the same flow equation, namely

$$\frac{dw}{d \ln \mu} = \epsilon w - \frac{3}{2} w^3. \quad (\text{B3})$$

In addition, we have to calculate the perturbative corrections to the bulk interaction vertex, which is identical to the usual $O(4)$ - ϕ^4 theory. In our convention the result is:

$$\frac{du}{d \ln \mu} = -2\epsilon u + 12u^2. \quad (\text{B4})$$

The hidden $O(4)$ symmetry of the theory becomes apparent upon writing the bosonic spinons as a 4-vector $(\Re z_\uparrow, \Im z_\uparrow, \Re z_\downarrow, \Im z_\downarrow)$.

Appendix C: FERMIONIC KONDO PROBLEM AT THE BAND EDGE

Remarkably, the two-level system coupled to the two-component bosonic gas studied in Sec. V turns out to

follow a weak-coupling RG flow identical to that of a fermionic Kondo problem, where the chemical potential is tuned to the (e.g. lower) band edge (i.e. with full particle-hole asymmetry). The equivalence can best be understood in terms of the local density of states – the only quantity which determines the impurity behavior – which in both cases (canonical bosons and fermions) is of the form $\rho(\omega) = \rho_0 |\omega|^r \theta(\omega)$.

The strict particle-hole asymmetry of the electrons implies that there are only particle excitations. Introducing dimensionless couplings according to standard practice⁷ we can derive the following flow equations for the fermionic problem:

$$\begin{aligned} \beta(j) &= rj - \frac{j^2}{2} + \frac{vj}{2}, \\ \beta(v) &= rv + \frac{3}{4}j^2 + \frac{1}{4}v^2, \end{aligned} \quad (\text{C1})$$

These equations are contained in the earlier analysis of Ref. 49, and are identical to those obtained for the problem of canonical bosons in Sec. V. Again, the equations are exact to all orders in perturbation theory (!).

For a general fermionic metallic ($r = 0$) Kondo problem with band asymmetry (i.e. the chemical potential not being pinned to the center of the band) one has to perform a two-step RG procedure: Initially, one has to follow the fully asymmetric scaling, Eq.(C1). Once the remainder of the band is symmetric, the usual poor man's scaling equations take over – here the potential scattering term is a marginal operator.

We note that the fully asymmetric fermionic Kondo problem can be relevant in the context of DMFT for Hubbard models: The transition from the undoped to the doped Mott insulator upon variation of the chemical potential happens precisely when the chemical potential reaches the gap edge (provided the transition is continuous).

¹ S. Sachdev, *Quantum Phase Transitions*, Cambridge University Press, Cambridge (1999).
² W. Metzner and D. Vollhardt, Phys. Rev. Lett. **62**, 324 (1989).
³ A. Georges, G. Kotliar, W. Krauth, and M. J. Rozenberg, Rev. Mod. Phys. **68**, 13 (1996).
⁴ D. Withoff and E. Fradkin, Phys. Rev. Lett. **64**, 1835 (1990).
⁵ A. C. Hewson, *The Kondo Problem to Heavy Fermions*, Cambridge University Press, Cambridge (1996).
⁶ C. Gonzalez-Buxton and K. Ingersent, Phys. Rev. B **57**, 14254 (1998).
⁷ L. Fritz and M. Vojta, Phys. Rev. B **70**, 214427 (2004).
⁸ L. Fritz, S. Florens, and M. Vojta, Phys. Rev. B **74**, 144410 (2006).
⁹ D. L. Cox and A. Zawadowski, Adv. Phys. **47**, 599 (1998).
¹⁰ R. M. Potok, I. G. Rau, H. Shtrikman, Y. Oreg, and D. Goldhaber-Gordon, cond-mat/0610721.

¹¹ B. A. Jones, C. M. Varma, and J. W. Wilkins, Phys. Rev. Lett. **61**, 125 (1988); B. A. Jones and C. M. Varma, Phys. Rev. B **40**, 324 (1989).
¹² I. Affleck, A. W. W. Ludwig, and B. A. Jones, Phys. Rev. B **52**, 9528 (1995).
¹³ G. Zaránd, C.-H. Chung, P. Simon, and M. Vojta, Phys. Rev. Lett. **97**, 166802 (2006).
¹⁴ M. Vojta, Phil. Mag. **86**, 1807 (2006).
¹⁵ A. J. Leggett, S. Chakravarty, A. T. Dorsey, M. P. A. Fisher, A. Garg, and W. Zwerger, Rev. Mod. Phys. **59**, 1 (1987).
¹⁶ M. Vojta, N.-H. Tong, and R. Bulla, Phys. Rev. Lett. **94**, 070604 (2005).
¹⁷ S. Sachdev, C. Buragohain, and M. Vojta, Science **286**, 2479 (1999).
¹⁸ M. Vojta, C. Buragohain, and S. Sachdev, Phys. Rev. B **61**, 15152 (2000).
¹⁹ S. Sachdev and M. Vojta, Phys. Rev. B **68**, 064419 (2003).

- ²⁰ M. Troyer, *Prog. Theor. Phys. Supp.* **145**, 326 (2002).
- ²¹ K. H. Höglund and A. W. Sandvik, *Phys. Rev. Lett.* **91**, 077204 (2003) and cond-mat/0701472.
- ²² J. L. Smith and Q. Si, *Europhys. Lett.* **45**, 228 (1999).
- ²³ A. M. Sengupta, *Phys. Rev. B* **61**, 4041 (2000).
- ²⁴ L. Zhu and Q. Si, *Phys. Rev. B* **66**, 024426 (2002).
- ²⁵ G. Zaránd and E. Demler, *Phys. Rev. B* **66**, 024427 (2002).
- ²⁶ M. Vojta and M. Kirčan, *Phys. Rev. Lett.* **90**, 157203 (2003).
- ²⁷ K. Le Hur, *Phys. Rev. Lett.* **92**, 196804 (2004) .
- ²⁸ S. Florens, L. Fritz, and M. Vojta, *Phys. Rev. Lett.* **96**, 036601 (2006).
- ²⁹ S. Sachdev and K. Park, *Annals of Physics (N.Y.)* **298**, 58 (2002).
- ³⁰ A. Recati, P. O. Fedichev, W. Zwerger, J. von Delft and P. Zoller, *Phys. Rev. Lett.* **94**, 040404 (2005).
- ³¹ T. Nikuni and J. E. Williams, *J. Low Temp. Phys.* **133**, 516 (2003).
- ³² A. V. Chubukov, T. Senthil, and S. Sachdev, *Phys. Rev. Lett.* **72**, 2089 (1994).
- ³³ S. V. Isakov, T. Senthil, and Y. B. Kim, *Phys. Rev. B* **72**, 174417 (2005).
- ³⁴ P. Azaria, P. Lecheminant, and D. Mouhanna, *Nucl. Phys. B* **455**, 648 (1995).
- ³⁵ S. Sachdev and T. Morinari, *Phys. Rev. B* **66**, 235117 (2002).
- ³⁶ A. Auerbach, *Interacting Electrons and Quantum Magnetism*, Springer (1994).
- ³⁷ E. Fradkin, *Field Theories of Condensed Matter Systems*, Addison-Wesley Publishing Company (1991).
- ³⁸ E. Fradkin and S. H. Shenker, *Phys. Rev. D* **19**, 3682 (1979).
- ³⁹ A. V. Chubukov and O. A. Starykh, *Phys. Rev. B*, **52**, 440 (1995).
- ⁴⁰ T. Senthil, L. Balents, S. Sachdev, A. Vishwanath, and M. P. A. Fisher, *Phys. Rev. B* **70**, 144407 (2004).
- ⁴¹ O. I. Motrunich and A. Vishwanath, *Phys. Rev. B* **70**, 075104 (2004).
- ⁴² A. Kolezhuk, S. Sachdev, R. R. Biswas, and P. Chen, *Phys. Rev. B* **74**, 165114 (2006).
- ⁴³ J. Zinn-Justin, *Quantum Field Theory and Critical Phenomena*, Oxford University Press (1996).
- ⁴⁴ Note that our notations for conjugate objects, \bar{b} and z^* , aim at distinguishing canonical bosons b from commuting numbers z . Of course, in the language of coherent-state path integrals the difference is in the dynamic term.
- ⁴⁵ A. Zawadowski and P. Fazekas, *Z. Physik* **226**, 235 (1969); P. Coleman, *Phys. Rev. B* **29**, 3035 (1984).
- ⁴⁶ T. A. Costi, J. Kroha, and P. Wölfle, *Phys. Rev. B* **53**, 1850 (1996).
- ⁴⁷ H.-J. Lee and R. Bulla, cond-mat/0606325.
- ⁴⁸ O. Bergman, *Phys. Rev. D* **46**, 5474 (1992).
- ⁴⁹ O. Ujsaghy, K. Vadar, G. Zarand, and A. Zawadowski, *J. Low Temp. Phys.* **126**, 1221 (2002).
- ⁵⁰ R. Coldea, D. A. Tennant, A. M. Tsvelik, and Z. Tylczynski, *Phys. Rev. Lett.* **86**, 1335 (2001).
- ⁵¹ R. Coldea, D. A. Tennant, and Z. Tylczynski, *Phys. Rev. B* **68**, 134424 (2003).
- ⁵² D. Binosi and L. Theussl, hep-ph/0309015 and <http://jaxodraw.sourceforge.net>.